Modulating Ligand Dissociation Through Methyl Isomerism in Accessory Sites: Binding of Retinol to Cellular Carriers

Carolina Estarellas,[†,§] Salvatore Scaffidi,[‡] Giorgio Saladino,[§] Francesca Spyrakis,[£] Lorella Franzoni,[¶] Carles Galdeano,[‡] Axel Bidon-Chanal,[,†] Francesco Luigi Gervasio,*[,§] and F. Javier Luque*[,†]*

[†] Department of Nutrition, Food Science and Gastronomy, Faculty of Pharmacy and Food Sciences, Institute of Biomedicine (IBUB) and Institute of Theoretical and Computational Chemistry (IQTCUB), University of Barcelona, 08921 Santa Coloma de Gramenet, Spain

[§] Department of Chemistry, University College London, London, UK

[‡] Department of Pharmacy, Pharmaceutical Technology, and Physical Chemistry, Faculty of Pharmacy and Food Science, and Institute of Biomedicine (IBUB), University of Barcelona, 08028 Barcelona, Spain

[£] Department of Drug Science and Technology, University of Turin, 10125 Turin, Italy

[¶] Department of Biomedical, Biotechnological and Translational Sciences, University of Parma, Parma, 43121 Parma, Italy

ABSTRACT

Due to the poor aqueous solubility of retinoids, evolution has tuned their binding to cellular proteins to address specialized physiological roles by modulating uptake, storage, and delivery to specific targets. With the aim to disentangle the structure-function relationships in these proteins and disclose clues for engineering selective carriers, the binding mechanism of the two most abundant retinol-binding isoforms was explored by using enhanced sampling molecular dynamics simulations and surface plasmon resonance. The distinctive dynamics of the entry portal site in the *holo* species was crucial to modulate retinol dissociation. Remarkably, this process is controlled at large extent by the replacement of Ile by Leu in the two isoforms, thus suggesting that a fine control of ligand release can be achieved through a rigorous selection of conservative mutations in accessory sites.

TOC GRAPHICS

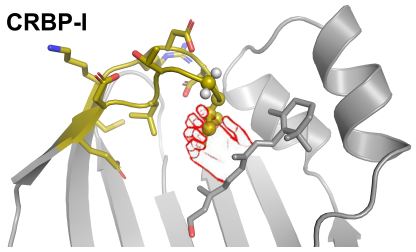

KEYWORDS

Free energy landscape, Ligand binding, Protein dynamics, Molecular recognition, Protein engineering

Retinol is essential for many physiological processes like cell growth and differentiation, morphogenesis, and vision.[1] However, the poor aqueous solubility makes the assistance of plasma and cellular binding proteins necessary for the delivery to target tissues, and the uptake and transport to specific partners in the cell.[2-4] In fact, the efficient transport of hydrophobic molecules has been solved by evolution through selection of specialized binding proteins, such as the calycin and SEC14-like superfamilies.[5-7] Although amino acid homology between the members of this widely distributed protein family is typically low, they share a similar β-barrel fold.[8,9] Many of these proteins contain only this structural domain and can presumably be involved in transport of hydrophobic compounds, while others may have other domains, reflecting the involvement in a variety of cellular functions, such as signal transduction and regulatory roles. Nevertheless, a precise knowledge of the mechanisms of recognition and binding is required to understand the roles in the cell, as illustrated by the ligand exchange mechanism that couples transfer of α-tocopherol and phosphatidylinositol phosphate lipids between the endosome and plasma membranes.[10,11]

The two most abundant intracellular retinol-binding proteins (CRBP; isoforms I and II) have distinct tissue distribution and binding affinity for retinol, reflecting the specialized adaptation of CRBP-I as retinol storage in the liver, and the uptake of retinol from the intestinal lumen and release into the blood by CRBP-II in epithelial cells.[4] The impact of residue substitutions selected by evolution in tuning the thermodynamics and kinetics of retinol binding to these isoforms is a conundrum. Hence, understanding the ability of CRBPs to sequester and protect retinol from the cellular milieu, and to direct it to dedicated targets is essential for furthering metabolic engineering through selective nanocarriers and for drug discovery in retinoid-related diseases.[12-14]

The structural fold of CRBP-I and II consists of a β-barrel formed by two almost orthogonal five-stranded β-sheets (A-E and F-J), and two short helices (αI and αII) inserted between βA and βB strands (Figure 1).[15] The entry portal site is a crucial element formed by helices αI and αII and turns βC-βD and βE-βF that enables retinol to enter into the cavity. Both NMR[15-17] and X-ray[18] data show that the binding mode of retinol is highly similar not only in human CRBP-I and II,

but also in rat CRBPs.[19-22] Despite the high structural identity between rat CRBP-I and II (56% residue identity and 70% residue homology), the retinol dissociation constant (K_D) for CBRP-I is smaller relative to CRBP-II, the ratio between binding affinities varying from ~100-fold[12] according to NMR measurements to 3.3-fold based on fluorimetric assays.[23] At present, it is unclear whether the affinity difference between the two isoforms stems from the few residue substitutions that line the binding pocket in the interior of the β-barrel (SI Figure S1), or alternatively to differences in the dynamics of CRBP-I and II,[15] which might affect the entry/release of retinol to/from the binding cavity.

To investigate the binding mechanisms in rat CRBP-I and II and explore their functional implications, a detailed analysis of *apo* and *holo* forms was performed by combining extended atomistic molecular dynamics (MD) simulations and parallel-tempering metadynamics (PT-metaD). We characterized the conformational flexibility of the two isoforms as well as the free energy surfaces for the opening/closing of the portal site in both *apo* and *holo* forms, and the formation/breaking of interactions between retinol and protein in the *holo* species. Furthermore, surface plasmon resonance (SPR) was used to examine the thermodynamics and kinetics of retinol binding. Overall, both theoretical and experimental results provide detailed insight into the binding mechanism, disclosing a linkage between retinol binding and the flexibility of the entry portal, particularly regarding the methyl isomerism between Ile and Leu in this accessory site of the two isoforms.

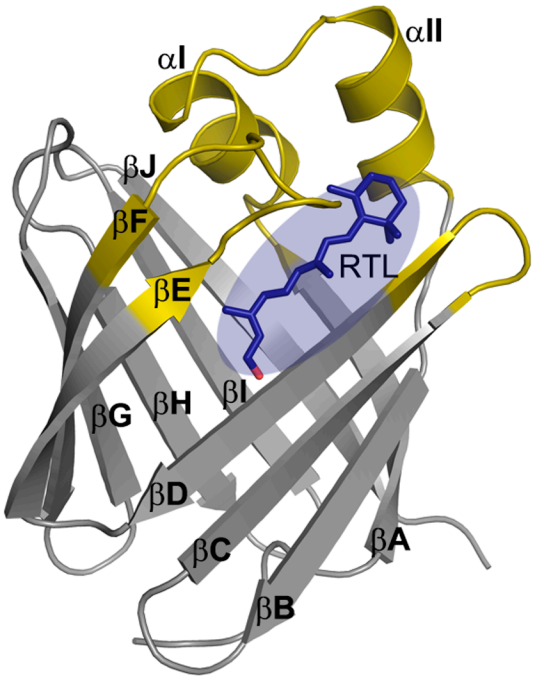

Figure 1. Representation of the retinol-CRBP complex. The structural fold of CRBP consists of 10 antiparallel β-strands (A-J) and two short α helices (I and II). The regions that define the entry portal site are highlighted in yellow. Retinol (RTL) is shown as blue sticks.

The conformational flexibility of *apo* and *holo* forms of CRBP-I and II was examined from three independent MD simulations (5, 3 and 3 μs) performed for each system, covering a total of 44 μs. The root-mean square deviation profiles supported the structural stability of the simulated systems along the trajectories (SI Figure S2). In both isoforms, the presence of retinol reduced the structural fluctuations of the protein, as expected from the interactions formed with residues in the binding cavity (Figure 2; see also SI Figures S3-S6). However, the pattern of residue fluctuations differed in the two isoforms. While *apo-I* showed increased fluctuations in loops βE-βF, βG-βH and at less extent βC-βD, *apo-II* exhibited larger fluctuations in helices αI-αII and at less extent in loops βC-βD and βD-βE (Figure 2A). Remarkably, most of these elements define the entry portal site, suggesting that the two isoforms differ in the dynamics of key structural elements implicated in the entry/release of retinol to/from the binding cavity.[24,25]

Essential Dynamics (ED) analysis was employed to gain insight into the distinct flexibility of CRBP-I and CRBP-II. The analysis was performed for the backbone atoms of residues 7–134 to avoid the noise due to the mobile parts at the N- and C-termini. The first essential mode (Figure 2B) accounted for 15-25% of the entire structural variance, and generally was 2-fold larger than the contribution explained by the second mode. The *apo* systems exhibited larger structural deformations, especially in the entry portal site, although helices αI-αII were stiffer in *apo-I* than in *apo-II*. On the other hand, *holo* systems were more rigid than their *apo* forms, as noted in the lower extent of the backbone motions. However, the decrease in conformational flexibility of the protein backbone did not affect similarly the two isoforms. In fact, the rigidification of the entry portal site was more important in *holo-I* than in *holo-II* (SI Table S1). At first sight, these results seemed to be in contrast with NMR H/F exchange experiments[15] that suggested a larger flexibility in both *apo* and *holo* states of CRBP-II relative to CRBP-I. However, it is worth noting that residues in the βE-βF loop of *apo-I* could not be assigned, while present results reveal that this structural element has a crucial influence on the dynamics of the portal site. Indeed, upon exclusion of the βE-βF loop in ED analyses, CRBP-II was slightly more flexible than CRBP-I in both *apo* and *holo* states (SI Table S1 and Figure S7), thus reconciling the experimental findings about the dynamics of the two isoforms and our results from MD simulations.

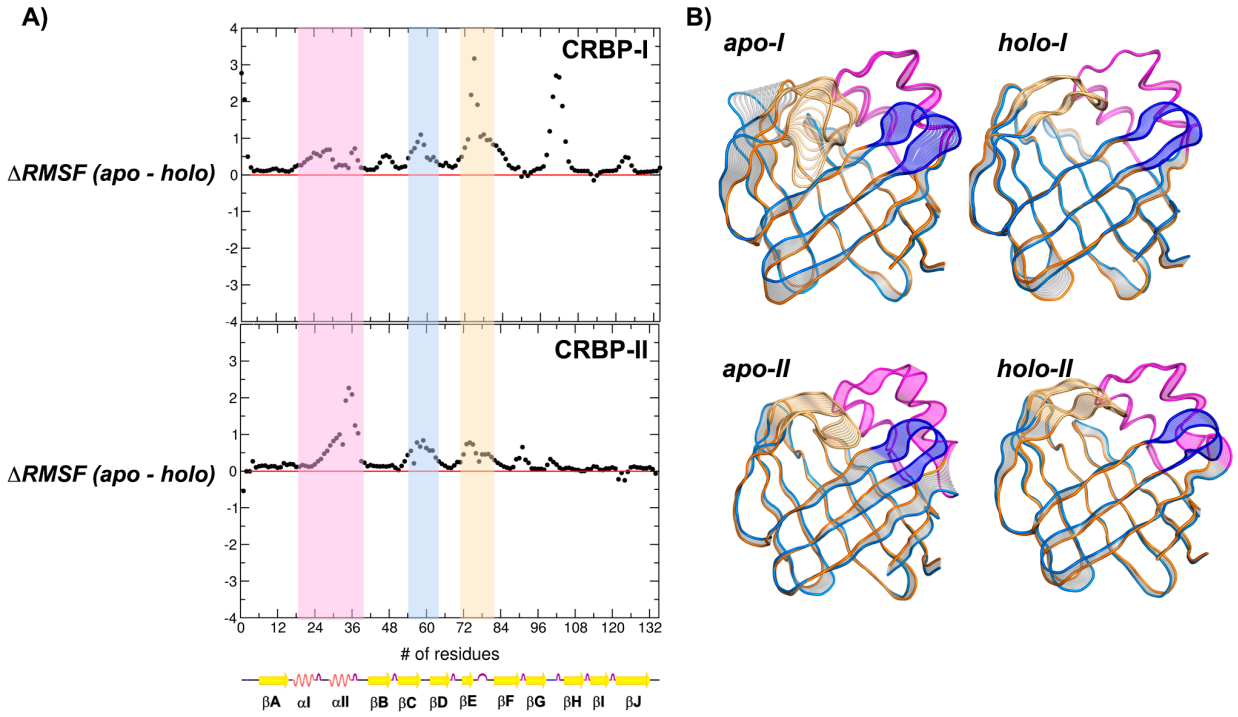

Figure 2. (A) Difference in residue fluctuations (ΔRMSF) observed along 5 μs MD trajectories between *apo* and *holo* states for (top) CRBP-I and (bottom) II. Highlighted regions correspond to structural elements of the entry portal site: helices αI and αII (magenta), loop βC-βD (blue), and loop βE-βF (orange). (B) Essential dynamics analysis of (top) CRBP-I and (bottom) II derived from the 5 μs MD simulation. Only the first projection of the whole system is shown for *apo* and *holo* forms.

To estimate the differences in the dynamics of *apo* and *holo* systems, the conformational entropy was evaluated for the whole system as well as separately for the entry portal site and the protein core, formed mainly by the β-barrel, using the procedure by Harris et al (See Supporting Information for details).[26] As expected, the results (Table 1; see also Table S2 and Figure S8) confirmed that *holo* systems were less flexible than *apo* ones, and pointed out that the decrease in entropy was larger for CRBP-I (0.56 Kcal mol^{-1} K^{-1}) than for CRBP-II (0.14 Kcal mol^{-1} K^{-1}). Furthermore, the conformational entropy (S^{vib}) obtained for *apo-I* was larger (by 0.35 Kcal mol^{-1} K^{-1}) than for *apo-II*, whereas the difference between the *holo* species was reduced to 0.07 Kcal mol^{-1} K^{-1}. Noteworthy, the entropy difference between *apo-I* and *apo-II* and between *holo-I* and *holo-II*

was mainly due to the differences in the entry portal site (*apo*: 0.27 Kcal mol^{-1} K^{-1}; *holo*: -0.06 Kcal mol^{-1} K^{-1}). Overall, these results confirm that the distinct patterns of conformational flexibility between the two isoforms primarily arise from the entry portal site.

Table 1. Entropy (S^{vib}) and entropy difference (ΔS) of the whole protein, and its core and entry portal site, determined from the analysis of the 5μs MD trajectory. Values (Kcal mol^{-1} K^{-1}) determined considering only the backbone atoms.

System	Protein[a]	Core[b]	Portal site[c]
S^{vib}(*apo-I*)[d]	2.97	1.76	1.21
S^{vib}(*holo-I*)	2.41	1.59	0.81
S^{vib}(*apo-II*)	2.62	1.68	0.94
S^{vib}(*holo-II*)	2.48	1.61	0.87
ΔS (*apo-I - holo-I*)	0.56	0.17	0.38
ΔS (*apo-II - holo-II*)	0.14	0.07	0.07
ΔS (*apo-I - apo-II*)	0.35	0.08	0.27
ΔS (*holo-I - holo-II*)	-0.07	-0.02	-0.06

[a] Residues 7-134. [b] Excluding the structural elements of the entry portal site. [c] Helices αI-αII and loops βC-βD and βE-βF. [d] The error of the conformational entropy was estimated from the standard deviation of S^{vib} obtained in the fitting at increasing simulation windows, with an upper value of 0.008 Kcal mol^{-1} K^{-1} for the whole protein and the portal site, and 0.005 Kcal mol^{-1} K^{-1} for the protein core.

Since the stiffness of the portal site in *holo-I* was higher than in *holo-II*, we hypothesized that the difference in binding affinity between CRBP-I and II might arise from a larger residence time of retinol in the former isoform. To address this question, PT-metaD was used to evaluate the free energy landscape for the opening/closing of the entry portal site in *apo* and *holo* systems, and the binding/unbinding of retinol to/from the *holo* systems. In order to take into account the larger structural flexibility of the open state compared to the closed one, the free energy change for the opening/closing of the entry portal site was estimated by averaging the values determined from three separate calculations, each relying on the use of distinct open structures chosen as

reference systems (SI Figures S9-S11). The results pointed out that the opening of the portal site in the *apo* state of CRBP-I and II was very similar and close to 5.5 ± 0.2 Kcal mol^{-1} (Figure 3A). However, the presence of retinol in the β-barrel had a marked influence on the opening of the portal site in *holo-I*, as this process was disfavoured by 3.8 Kcal mol^{-1} compared to *apo-I*. Remarkably, the presence of retinol led to a modest increase in the cost of opening the portal site in *holo-II* (by only 0.7 Kcal mol^{-1}) relative to *apo-II*. These findings agree with the larger decrease in conformational entropy found for CRBP-I relative to CRBP-II upon retinol binding (see above and Table 1).

The analysis of the structures sampled during the opening of the portal site reveals that there is a slight rearrangement of retinol in the binding pocket, although the ligand remains trapped in the interior of the β-barrel after opening of the loop in both CRBP-I and II (Figure 4). However, whereas the rearrangement of retinol occurs in a fast process during the first 100 ns of the loop opening for CRBP-II, a slower process that involves a gradual rearrangement of retinol is observed for the loop opening in CRBP-I. This suggests the presence of stronger interactions between the ligand with the residues of the portal site in this latter isoform, as will be discussed later.

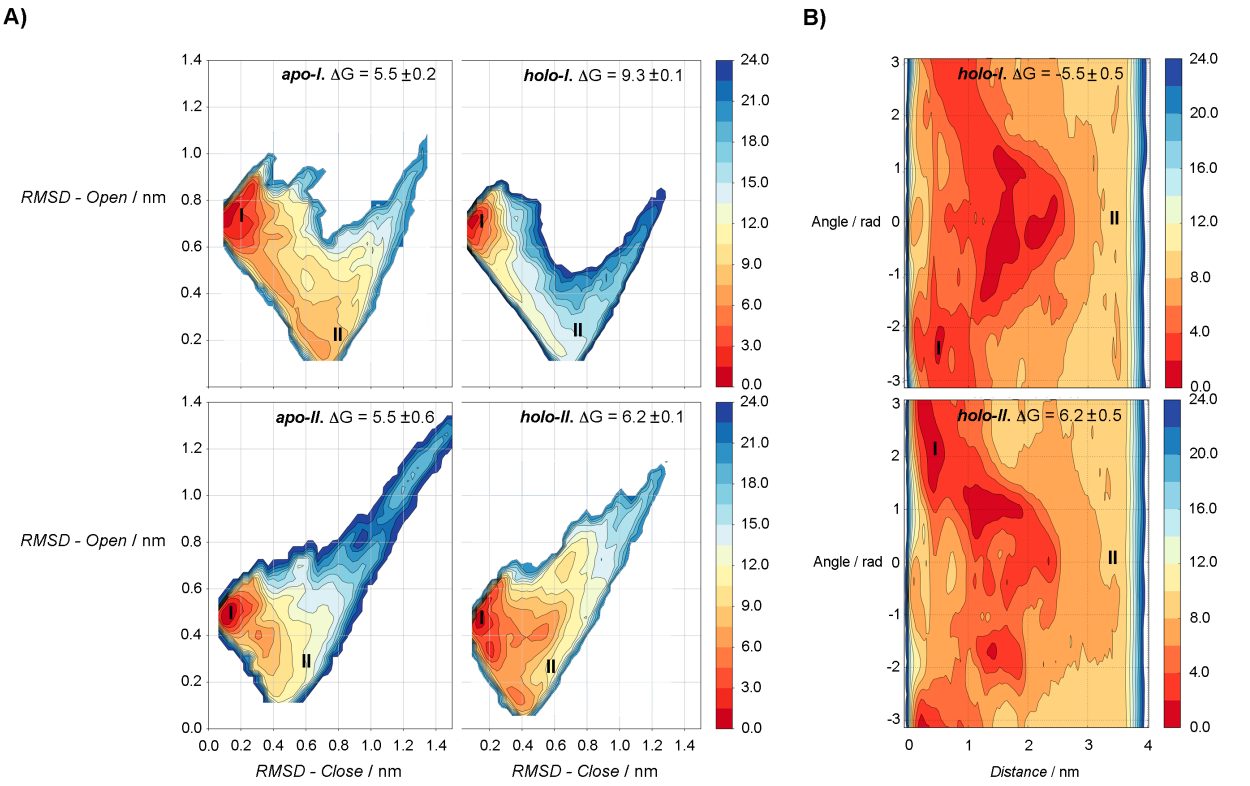

Figure 3. (A) Free energy surface for the opening/closing of the entry portal site in *apo* and *holo* forms of CRBP-I and II. Closed and open states are indicated by symbols I and II, respectively. Contour lines are drawn every 1.5 Kcal mol^{-1}. Values in the plots are the average of three estimates generated by using different reference structures for the open state. (B) Free energy surface for the binding/unbinding of retinol from *holo-I* and *holo-II*. Bound and unbound states are indicated by symbols I and II, respectively. Contour lines are drawn every 2 Kcal mol^{-1}.

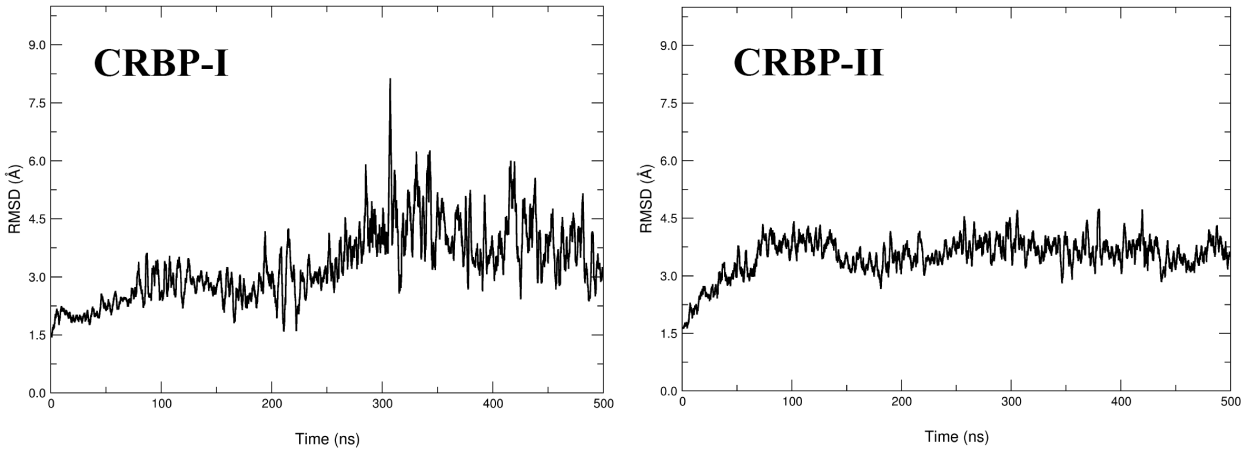

Figure 4. RMSD (Å) of retinol along the opening of the portal site in (left) CRBP-I and (right) II. The RMSD was determined relative to the arrangement of retinol in the energy-minimized structure of *holo-I* and *holo-II* species, after alignment of the protein core. The snapshots were taken during the 500 ns of the pT-metaD simulation at 300 K.

PT-MetaD simulations were also used to estimate the free energy for retinol binding/unbinding from the open state of the two isoforms. Calculations were started from suitably chosen *holo* structures characterized by the presence of a portal site open enough to enable the release of retinol from the protein cavity without steric clashes. Similar events were involved in the release of retinol from CRBP-I and II (SI Figure S12). Briefly, retinol unbinding involves first the breakage of the hydrogen bond formed by the terminal hydroxyl group and subsequent release of the polyene tail, which becomes progressively more exposed to water molecules, followed by the breakage of the van der Waals interactions with the β-ionone ring, leading to immersion in the aqueous environment. The free energy surfaces determined for CRBP-I and II (Figure 3B) pointed out that the energetic cost for retinol unbinding is only 1 Kcal mol^{-1} higher in *holo-II*.

Overall, the combination of the free energy estimates obtained for the opening/closing in *apo* and *holo* states, and the binding/unbinding of retinol from *holo* species, indicates that the affinity of CRBP-I for retinol is 2.4 Kcal mol^{-1} more favourable relative to CRBP-II (Figure 5). Noteworthy, this agrees with the experimentally observed greater affinity of retinol for CRBP-I, as the predicted affinity lies between the range of experimental values, which vary from an upper

threshold of <~100-fold[12] to a lower limit of 3.3-fold greater affinity for CRBP-I.[23] Remarkably, our results also revealed that the difference in binding affinity is mainly determined by the opening/closure of the entry portal site in the *holo* state. This suggests that the larger cost of opening the *holo-I* complex cannot be attributed to the interactions formed by the portal site with the rest of the protein, as the free energy changes determined for the opening of the portal site in the *apo* species are highly similar in the two isoforms (Figure 5; see also SI Figure S13). Therefore, it may be speculated that the interactions formed between retinol and the entry portal site in the *holo* species are more favourable in CRBP-I than in CRBP-II, thus providing a basis to justify the larger decrease in conformational flexibility observed upon retinol binding to CRBP-I relative to CRBP-II.

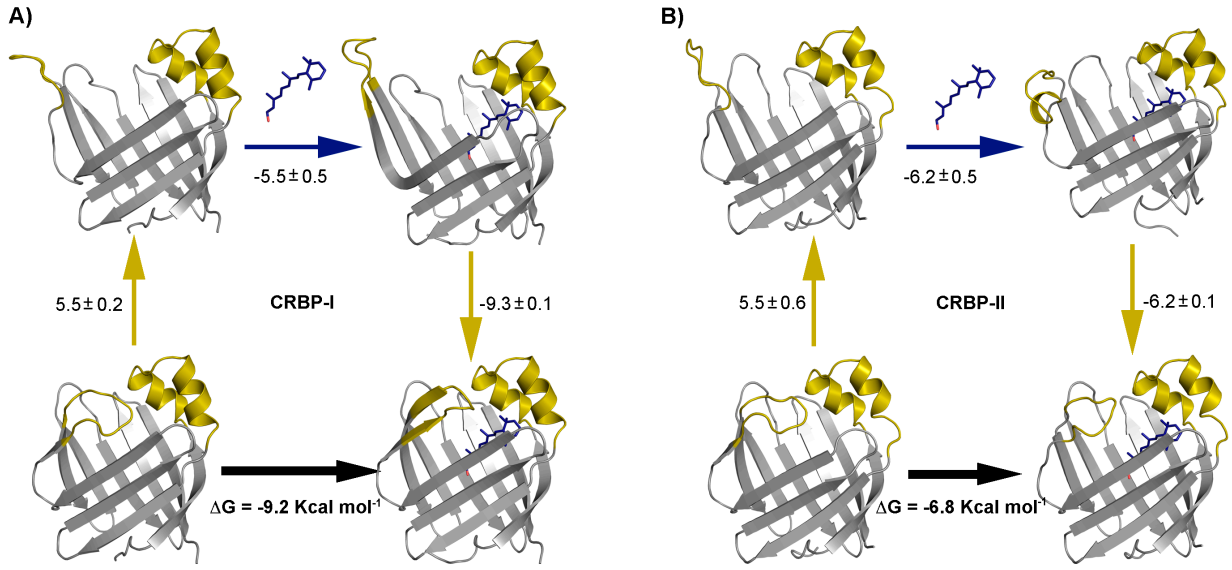

Figure 5. Thermodynamic cycle for the opening of the entry portal site for *apo* states, the binding of retinol, and the closure of the portal site in *holo* systems in (A) CRBP-I and (B) II. Values are in Kcal mol^{-1}.

This assumption was confirmed from the analysis of the interaction energies between retinol and the structural elements that define the portal site in *holo-I* and *holo-II* (Table 2). Whereas the interaction energy with helices αI-αII and loop βC-βD was similar in the two *holo* systems, the interaction of retinol with loop βE-βF was 2.6 Kcal mol^{-1} more stabilizing in *holo-I*. Further

decomposition into pairwise ligand-residue contributions revealed that the energy difference was mainly due to the interactions with Gly77 and Ile78 in CRBP-I, which were 2.1 Kcal mol^{-1} more stabilizing than the interactions with Gly77 and Leu78 in CRBP-II (SI Table S3). In contrast, other residue substitutions located in the loop βE-βF contributed less than 0.2 Kcal mol^{-1}, even though this can be justified from either the solvent-exposed arrangement of the side chain of these residues or the large distance from the mutated residue to retinol. In contrast, residues at position 78 (Ile in CRBP-I, Leu in CRBP-II) are located at the top of the loop βE-βF, pointing toward the interior of the β-barrel, and form van der Waals contacts with the β-ionone ring and the unsaturated chain of retinol (Figure 6). Overall, these results point out that the difference in the interaction energy with retinol can be mainly attributed to the conservative mutation of Ile78 in CRBP-I to Leu78 in CRBP-II, disclosing an unexpected effect related to the methyl isomerism between the side chains of these two residues.

To confirm the impact of the Ile/Leu mutation at position 78 on the binding of retinol to CRBP-I and II, SPR was used to characterize the kinetic rate constants for the association (k_{on}) and dissociation (k_{off}) of retinol to CRBP-II and its Leu78→Ile single-mutated variant (SI Figures S14-S15 and Table S4). The results show that the k_{on} remains essentially unaltered for both CRBP-II and the mutated variant (Table 3). However, the k_{off} of retinol is slowed down by a factor of ~2.2 in the mutated protein. The increased residence time originated by the single-point mutation Leu78 →Ile agrees with the expected strengthening of the interaction of retinol with the mutated residue in CRBP-I (Ile) relative to CRBP-II (Leu), as deduced from the PT-metaD simulations and the decomposition analysis presented above (Table 2 and SI Table S3). Furthermore, the dissociation constant (K_D) is decreased by ~2.8-fold in the mutated CRBP-II, which compares with the lower limit of the experimental ratio between CRBP-I and CRPB-II (~3.3-fold).[23]

Table 2. Interaction energies (E_{int}; Kcal mol^{-1}) and its electrostatic (E_{ele}; Kcal mol^{-1}) and van der Waals (E_{vdw}) components between retinol and the entry portal site for *holo-I* and *holo-II*.

System[a]	E_{int}	E_{ele}	E_{vdw}
holo-I (αI-αII)	-10.6	0.2	-10.8
holo-II (αI-αII)	-11.0	-0.4	-10.6
holo-I (βC-βD)	-6.4	0.1	-6.5
holo-II (βC-βD)	-6.0	0.3	-6.3
holo-I (βE-βF)	-6.4	-0.2	-6.2
holo-II (βE-βF)	-3.8	-0.4	-3.4

[a] Calculations performed for 50 snapshots taken regularly in the last microsecond of the 5μs MD simulations. Helices α-I and α-II comprise residues Glu15-Leu37, and loops βC-βD and βE-βF involve residues Ser55-Asn59 and Glu73-Cys/Val83, respectively.

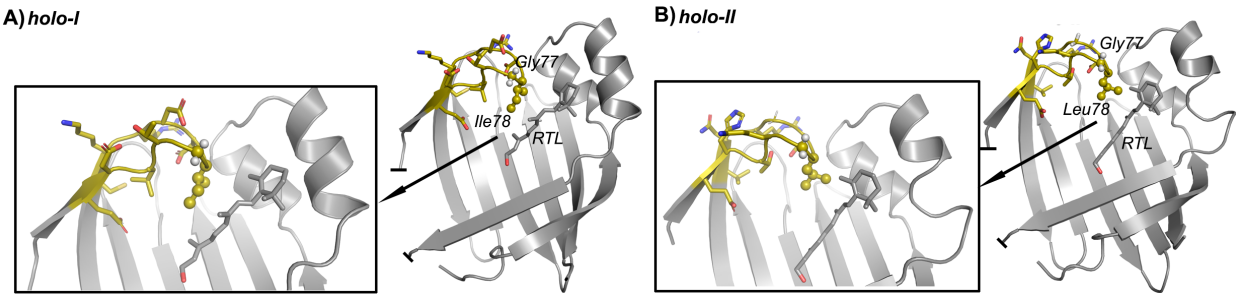

Figure 6. Representation of (A) holo-I and (B) holo-II. Residues in the βE-βF loop with higher contribution to the interaction energy with retinol (RTL) are highlighted as spheres, and retinol is shown as sticks (β-sheets C and D are not shown for the sake of clarity).

Table 3. Kinetic rate constants (k_{on}, M^{-1} s^{-1}; k_{off}, s^{-1}) and dissociation constant (K_D; M) for the interactions between retinol and CRBP-II and its Leu78→Ile single-mutated variant.

CRBP-II	k_{on}	k_{off}	K_D
wild type	241.5	$17.9\ 10^{-3}$	$7.4\ 10^{-5}$
Leu78→Ile	312.4	$8.1\ 10^{-3}$	$2.6\ 10^{-5}$

The selectivity of different members of cytosolic binding proteins toward distinct retinoid-like compounds has been related to the presence of specific residues in the β-barrel.[27,28] Furthermore, other studies have identified hydrophobic contacts between ligands and structural elements of the mobile gate in SEC14-like family members.[29-31] Present results, however, point out that a seemingly minor chemical change related to the methyl isomerism between Ile and Leu at the portal site modulates the binding properties of retinol between closely related CRBP isoforms. The net effect is the enhanced free energy penalty associated to the closed→open transition, which would disfavour the release of the ligand and increase the residence time of retinol in the interior of the β-barrel. Noteworthy, the affinity for the two isoforms is finely modulated by the differential interaction of the β-ionone unit of retinol with the residue (Ile/Leu) at the top of the loop βE-βF, suggesting an unexpected role of the methyl isomerism between the two similar residues.

From a functional point of view, these results unveil a subtle regulation mechanism that underlies the distinct physiological role of the two isoforms. In enterocytes, CRBP-II plays an important, but not essential, role in assisting the transient exchange of retinol from the intestinal lumen to the lymph, making it necessary to have an efficient delivery system. In contrast, CRBP-I is highly expressed in hepatic cells, where it participates in the storage of retinol and controls its mobilization to ensure a steady supply in the blood plasma. Therefore, the strengthened interaction of retinol with the β-barrel lid may have evolved as a mechanism to self-regulate long-term retinol mobilization subject to specific requirements of active retinoid metabolites to the target cells without being affected by the fluctuations of the dietary intake.

Finally, these findings demonstrate that conservative changes in specific residues at remote sites distinct from the binding pocket, which should not alter the gross structural and physicochemical features of the protein, may result in a fine-tuning of the ligand's binding properties. Thus, a thoughtful selection of residue variations may be instrumental for engineering a gradual evolution of structure-function relationships in nanomolecular devices.

ASSOCIATED CONTENT

Supporting Information. Additional results for the structural, dynamical and energetic analysis of the retinol-carrier proteins, results from SPR assays, and description of theoretical and experimental methods.

AUTHOR INFORMATION

Corresponding Author

* E-mail: abidonchanalb@ub.edu (A.B.-C.).

* E-mail: f.l.gervasio@ucl.ac.uk (F.G.).

* E-mail: fjluque@ub.edu (F.J.L.).

ORCID

Carolina Estarellas: 0000-0002-0944-9053

Salvatore Scaffidi: 0000-0002-9067-5700

Giorgio Saladino: 0000-0002-3234-5762

Francesca Spyrakis: 0000-0002-4016-227X

Lorella Franzoni: 0000-0003-3039-5843

Carles Galdeano: 0000-0003-1702-0369

Axel Bidon-Chanal: 0000-0002-1666-1490

Francesco L. Gervasio: 0000-0003-4831-5039

F. Javier Luque: 0000-0002-8049-3567

Notes

The authors declare no competing financial interests.

ACKNOWLEDGMENT

We thank the Ministerio de Economía y Competitividad (MINECO: SAF2017-88107-R, SAF2015-68749-R; AEI/FEDER UE) and the Generalitat de Catalunya (2017SGR1746) for financial support, the Barcelona Supercomputing Center (BSC; BCV-2013-1-0016 and BCV-2013-2-0016), PRACE (BSC; 2010PA3167) and HEcBiosim (EPSRC EP/R029407/1) for computational resources. G.S. and F.L.G. acknowledge EPSRC (EP/M013898/1; EP/P022138/1; EP/P011306/1) for financial support. S.C. acknowledges University of Barcelona for APIF fellowship. C.E. thanks MINECO for postdoctoral fellowship (FPDI-2013-15572) and funding from the EU Horizon 2020 research and innovation programme under the Marie Skłodowska-Curie grant agreement No. 795116.

REFERENCES

(1) Blomhoff, R.; Blomhoff, H. K. Overview of Retinoid Metabolism and Function. *J. Neurol.* **2006**, *66*, 606–630.

(2) Olson, C. R.; Mello, C. V. Significance of Vitamin A to Brain Function, Behavior and Learning**.** *Mol. Nutr. Food Res.* **2010**, *54*, 489–495.

(3) N. M. Bass, N. M. Cellular Binding Proteins for Fatty Acids and Retinoids: Similar or Specialized Functions? *Mol. Cell. Biochem.* **1993**, *123*, 191–202.

(4) Napoli, J. L. Cellular Retinoid Binding-Proteins, CRBP, CRABP, FABP5: Effects on Retinoid Metabolism, Function and Related Diseases. *Pharmacol. Ther.* **2017**, *173*, 19–33.

(5) Schaap, F. G.; van der Vusse, G. J.; Glatz, J. F. C. Evolution of the Family of Intracellular Lipid Binding Proteins in Vertebrates. *Mol. Cell. Biochem.* **2002**, *239*, 69–77.

(6) Saito, K.; Tautz, L.; Mustelin, T. The Lipid-Binding SEC14 Domain. *Biochim. Biophys. Acta.* **2007**, *1771*, 719–726.

(7) Bankaitis, V. A.; Mousley, C. J.; Schaaf, G. The Sec14-Superfamily and Mechanisms for Crosstalk Between Lipid Metabolism and Lipid Signalling. *Trends Biochem. Sci.* **2010**, *35*, 150–160.

(8) Sato, Y.; Arai, H.; Miyata, A.; Tokita, S.; Yamamoto, K.; Tanabe, T.; Inoue, K. Primary Structure of alpha-Tocopherol Transfer Protein from Rat Liver. Homology with Cellular Retinaldehyde-Binding Protein. *J. Biol. Chem.* **1993**, *268*, 17705–17710.

(9) Sha, B.; Philips, S. E.; Bankaitis, V. A.; Luo, M. Crystal Structure of the Saccharomyces cerevisiae Phosphatidylinositol-Transfer Protein. *Nature* **1998**, *391*, 506–510.

(10) Kono, N.; Ohto, U.; Hiramatsu, T.; Urabe, M.; Uchida, Y.; Satow, Y.; Arai, H. Impaired α-TTP-PIPs Interactions Underlies Familial Vitamin E Deficiency. *Science* **2013**, *340*, 1106–1110.

(11) Lamprakis, C.; Stocker, A.; Cascella, M. Mechanisms of Recognition and Binding of a-TTP to the Plasma Membrane by Multi-Scale Molecular Dynamics Simulations. *Front. Mol. Biosci.* **2015**, *2*, 36.

(12) Li, E.; Qian, S. J.; Winter, N. S.; Avignon, A.; Levin, M. S.; Gordon, J. I. Fluorine Nuclear Magnetic Resonance Analysis of the Ligand Binding Properties of Two Homologous Rat Cellular Retinol-Binding Proteins Expressed in *Escherichia coli*. *J. Biol. Chem.* **1991**, *266*, 3622–3629.

(13) Eriksson, U.; Das, K.; Busch, C.; Nordlinder, H.; Rask, L.; Sundelin, J.; Sällström, J.; Peterson, P. A. Cellular Retinol-Binding Protein. Quantitation and Distribution. *J. Biol. Chem.* **1984**, *259*, 13464–13470.

(14) Bushue, N.; Wan, Y. J. Retinoid Pathway and Cancer Therapeutics. *Adv. Drug Deliv. Rev.* **2010**, 62, 1285–1298.

(15) Franzoni, L.; Lücke, C.; Pérez, C.; Cavazzini, D.; Rademacher, M.; Ludwig, C.; Spisni, A.; Rossi, G. L.; Rüterjans, H. Structure and Backbone Dynamics of Apo- and Holo-Cellular Retinol-Binding Protein in Solution. *J. Biol. Chem.* **2002**, *277*, 21983–21997.

(16) Lu, J.; Lin, C. L.; Tang, C.; Ponder, J. W.; Kao, J. L.; Cistola, D. P.; Li, E. Binding of Retinol Induces Changes in Rat Cellular Retinol-Binding Protein II Conformation and Backbone Dynamics. *J. Mol. Biol.* **2000**, *300*, 619–632.

(17) Lu, J.; Cistola, D. P.; Li, E. Two Homologous Rat Cellular Retinol-Binding Proteins Differ in Local Conformational Flexibility. *J. Mol. Biol.* **2003**, *330*, 799–812.

(18) Winter, N. S.; Bratt, J. M.; Banaszak, L. J. Crystal Structures of Holo and Apo-Cellular Retinol-Binding Protein II. *J. Mol. Biol.* **1993**, *230*, 1247–1259.

(19) Silvaroli, J. A.; Arne, J. M.; Chelstowska, S.; Kiser, P. D.; Banerjee, S.; Golczak, M. Ligand Binding Induces Conformational Changes in Human Cellular Retinol-Binding Protein 1 (CRBP1) Revealed by Atomic Resolution Crystal Structures. *J. Biol. Chem.* **2016**, *291*, 8528–8540.

(20) Menozzi, I.; Vallese, F.; Polverini, E.; Folli, C.; Berni, R.; Zanotti, G. Structural and Molecular Determinants Affecting the Interaction of Retinol with Human CRBP1. *J. Struct. Biol.* **2017**, *197*, 330–339.

(21) Nossoni, Z.; Assar, Z.; Yapici, I.; Nosrati, M.; Wang, W.; Berbasova, T.; Vasileiou, C.; Borhan, B.; Geiger, J. Structures of Holo Wild-Type Human Cellular Retinol-Binding Protein II (hCRBPII) Bound to Retinol and Retinal. *Acta Crystallogr. Sect. D* **2014**, *70*, 3226–3232.

(22) Tarter, M.; Capaldi, S.; Carrizo, M. E.; Ambrosi, E.; Perduca, M.; Monaco, H. L. Crystal Structure of Human Cellular Retinol-Binding Protein II to 1.2 Å Resolution. *Proteins* **2008**, *70*, 1626–1630.

(23) Kane, M. A.; Bright, F. V.; Napoli, J. L. Binding Affinities of CRBPI and CRBPII for 9-*cis*-Retinoids. *Biochim. Biophys. Acta* **2011**, *1810*, 514–518.

(24) Franzoni, L.; Cavazzini, D.; Rossi, G. L.; Lücke, C. New Insights on the Protein-Ligand Interaction Differences Between the Two Primary Cellular Retinol Carriers. *J. Lipid Res.* **2010**, *51*, 1332–1343.

(25) Mittag, T.; Franzoni, L.; Cavazzini, D.; Schaffhausen, B.; Rossi, G. L.; Günther, U. L. Retinol Modulates Site-Specific Mobility of Apo-Cellular Retinol-Binding Protein to Promote Ligand Binding. *J. Am. Chem. Soc.* **2006**, *128*, 9844–9848.

(26) Harris, S. A.; Gavathiotis, E.; Searle, M. S.; Orozco, M.; Laughton, C. A. Cooperativity in Drug-DNA Recognition: A Molecular Dynamics Study. *J. Am. Chem. Soc.* **2001**, *123*, 12658–12663.

(27) Helbling, R. E.; Bolze, C. S.; Golczak, M.; Palczewski, K.; Stocker, A.; Cascella, M. Cellular Retinaldehyde Binding Protein—Different Binding Modes and Micro-Solvation Patterns for High-Affinity 9-*cis*- and 11-*cis*-Retinal Substrates. *J. Phys. Chem. B* **2013**, *117*, 10719–10729.

(28) Bolze, C. S.; Helbling, R. E.; Owen, R. L.; Pearson, A. R.; Pompidor, G.; Dworkowski, F.; Fuchs, M. R.; Furrer, J.; Golczak, M.; Palczewski, K.; Cascella, M.; Stocker, A. Human Cellular Retinaldehyde-Binding Protein Has Secondary Thermal 9-*cis*-Retinal Isomerase Activity. *J. Am. Chem. Soc.* **2014**, *136*, 137–146.

(29) Meier, R.; Tomizaki, T.; Schulze-Briese, C.; Baumann, U.; Stocker, A. The Molecular Basis of Vitamin E Retention: Structure of Human a-Tocopherol Transfer Protein. *J. Mol. Biol.* **2003**, *331*, 725–734.

(30) He, X.; Lobsiger, J.; Stocker, A. Bothnia Distrophy is Caused by Domino-Like Rearrangements in Cellular Retinaldehyde-Binding Protein Mutant R234W. *Proc. Natl. Acad. Sci. USA* **2009**, *106*, 18545-18550.

(31) Christen, M.; Marcaida, M. J.; Lamprakis, C.; Aeschimann, W.; Vaithiligam, J.; Schneider, P.; Hilbert, M.; Scheneider, G.; Cascella, M.; Stocker, A. Structural Insights on Cholesterol Endosynthesis: Binding of Squalene and 2,3-Oxidosqualene to Supernantant Protein Factor. *J. Struct. Biol.* **2015**, *190*, 261-270.